M5 Model Tree and Gene Expression Programming Based Modeling of Sandy Soil Water Movement under Surface Drip

Article · January 2014

CITATIONS
17

READS
248

3 authors:

Saeed Samadianfard
University of Tabriz
55 PUBLICATIONS **1,004** CITATIONS
SEE PROFILE

Ali Ashraf Sadraddini
University of Tabriz
76 PUBLICATIONS **732** CITATIONS
SEE PROFILE

Amir Hossein Nazemi
University of Tabriz
52 PUBLICATIONS **893** CITATIONS
SEE PROFILE

Agric. sci. dev., Vol(3), No (5), May, 2014. pp. 178-190

TI Journals
Agriculture Science Developments
www.tijournals.com

ISSN:
2306-7527

M5 Model Tree and Gene Expression Programming Based Modeling of Sandy Soil Water Movement under Surface Drip Irrigation

Saeed Samadianfard *
Department of Water Engineering, Faculty of Agriculture, University of Tabriz, Iran

Amir Hossein Nazemi
Department of Water Engineering, Faculty of Agriculture, University of Tabriz, Iran

Ali Ashraf Sadraddini
Department of Water Engineering, Faculty of Agriculture, University of Tabriz, Iran

**Corresponding author:* s.samadian@tabrizu.ac.ir

Keywords

Artificial intelligence
Data mining technique
Infiltration
Numerical models
Pore network modeling

Abstract

Drip irrigation has a priority in selecting an appropriate irrigation method because of its potential of precisely applying water at the requested quantity and position through a field. A proper design and management of a drip irrigation system is dependent upon a better understanding of wetting patterns and water distribution in soil. This paper examines the potential of gene expression programming (GEP), which is a variant of genetic programming (GP), and M5 model tree in simulating wetting patterns of drip irrigation. First by considering 10 sandy soils of various sand percentages, soil wetting patterns for different emitter discharges and durations of irrigation have been simulated by using pore network modeling conjuncted by Richards' equation (PNMCRE). Then using the calculated values of depth and radius of wetting pattern as target outputs, GEP and M5 model trees have been considered. Results showed that in estimation of radius and depth of wetting patterns, the M5 model tree had better agreement than GEP with results of PNMCRE model in terms of some statistical criteria. Also, laboratory experimental results in a sandy soil with emitter discharge of 4 L/h showed reasonable agreement with M5 model tree results. Finally it can be concluded on the basis of the results of this study that M5 model tree appears to be a promising technique for estimating wetting patterns of drip irrigation.

1. Introduction

Agriculture, which is one of the economic sectors that uses the most freshwater, is under great pressure to improve the efficiency of its use of this resource. To this end, drip irrigation is potentially the most efficient irrigation system in terms of water use, although to reach its full potential irrigation management also needs to be carried out in a rational manner [1]. On the other hand, the information on depth and radius of wetted zone of soil under surface application of water plays a great significant role in designing and management of surface drip irrigation system in supplying the required amount of water to the plant [2].

Mathematical models have been proven very useful in predicting water and nutrient movement in the soil [3] enabling improved drip irrigation system design and management. Philip [4] developed a mathematical theory for a two- and three-dimensional unsaturated water flow from buried point sources and spherical cavities. Ben-Asher and Phene [5] presented a numerical model to analyze two-dimensional water flow for surface and subsurface drip systems.

Numerical methods also have been developed to simulate the mentioned phenomenon [6,7]. Skaggs et al. [8] demonstrated that HYDRUS-2D simulations of drip irrigation were in agreement with detailed field measurements. Zhou et al. [9] compared experimental observations with the HYDRUS 2D and APRI model in a vineyard under alternate partial root zone drip irrigation and concluded that APRI-model was more suitable for modeling the soil water dynamics in the arid region with greater soil evaporation and uneven root distribution. Li et al. [10] also used the HYDRUS-2D model to simulate wetting dimensions of soil volume and distributions of water content and nitrate concentrations in soil and compared them with data obtained from laboratory experiments conducted on loam and sandy soils. An excellent agreement was obtained between the simulated results and the measured data.

Pore-scale modeling has been widely used as a platform to study multiphase flow in petroleum engineering, hydrology and environment engineering [11,12] and offers an alternative to empirical models. Pore-scale or network models can be used to predict multiphase flow behavior by simulating the flow process based on a detailed description of the pore structure, fluid characteristics, and the governing pore-scale displacement mechanisms. The pore space in a porous medium is represented by a network of pores (corresponding to the larger void spaces) and throats (the narrow openings connecting the pores) with parameterized geometries and topology through which multiphase flow can be simulated. Held and Celia [13] used network modeling to compute relationships between capillary pressure, saturation and interfacial areas. Joekar-Niasar et al. [14] used a tube network model, in which zero volume was assigned to the nodes, as well as a sphere-and-tube model to study the water – air interfacial area relationships with capillary pressure and saturation in two-phase systems through primary drainage and imbibition simulations.

Gene expression programming (GEP) has been applied to a wide range of problems in artificial intelligence, artificial life, engineering and science, financial markets, industrial, chemical and biological processes, and mechanical models including symbolic regression, multi-agent strategies, time series prediction, circuit design and evolutionary neural networks. GEP can be successively applied to areas where (i) the interrelationships among the relevant variables are poorly understood (or where it is suspected that the current understanding may be wrong), (ii) finding the size and shape of the ultimate solution is difficult and a major part of the problem, (iii) conventional mathematical analysis does

Agriculture Science Developments Vol(3), No (5), May, 2014.

not, or cannot, provide analytical solutions, (iv) an approximate solution is acceptable (or is the only result that is ever likely to be obtained), (v) small improvements in performance are routinely measured (or easily measurable) and highly prized, (vi) there is a large amount of data in computer readable form, that requires examination, classification, and integration, e.g., molecular biology for protein and DNA sequences, astronomical data, satellite observation data, financial data, marketing transaction data, or data on the World Wide Web [15]. In the last decade, genetic programming (GP) has been used as a viable alternative approach to physical models [16,17,18].

Within the last decade, several studies have reported the use of M5 model tree as a decision tree based regression approach for water resource applications [19,20,21]. Ditthakit and Chinnarasri [22] presented a derivation of new pan coefficient equations for Class A pan and Colorado sunken pan by using the M5 model tree based on data mining techniques.

Although numerical and mathematical models offer higher flexibility to more realistically represent natural flow systems, they require expertise to implement and can be computationally intensive reducing the application of numerical models for irrigation system design and management decision-making [23]. The goal of this study is to propose an alternative way for computation of the spatial and temporal wetting patterns during infiltration from surface drip emitters based on M5 model trees and gene expression programming models, using the data produced by dynamic pore network modeling and solving partial differential Richards' equation by finite difference scheme.

2. Methodology

2.1. Dynamic pore network model

In this research we have used a dynamic pore network model proposed by Joekar-Niasar et al. [24]. The mentioned pore network model has a three-dimensional regular lattice structure with fixed coordination number of six. Pore bodies have cubic shape and pore throats have square cross sections. Figure 1 shows a schematic presentation of two pore bodies and the connected pore throat. Additional details about dynamic pore network model can be found in Joekar-Niasar et al. [24].

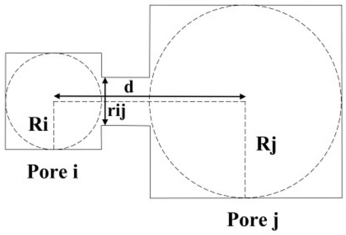

Figure 1. Schematic presentation of two pore bodies and the connected pore throats

2.2. Numerical solving of Richards' equation using finite difference scheme

The Richards' equation is the most general method to compute soil moistures and hydrological fluxes, such as infiltration in porous media. Consider two - and/or three-dimensional isothermal uniform Darcian flow of water in a variably saturated rigid porous medium and assume that the air phase plays an insignificant role in the liquid flow process. The governing flow equation for these conditions is given by the following modified form of the Richards' equation [25]:

$$C\frac{\partial h}{\partial t}=\frac{1}{r}\frac{\partial}{\partial r}\left(rK(h)\frac{\partial h}{\partial r}\right)+\frac{\partial}{\partial z}\left(K(h)\frac{\partial h}{\partial z}\right)-\frac{\partial K}{\partial z}-S(r,z,t,h) \tag{1}$$

where C= specific capacity of water [1/L], h= pressure head [L], r, z= radial and vertical directions, t= time [T], S= sink term [1/T] and K= unsaturated hydraulic conductivity function [L/T].

The general form of Richards' equation after discretization, linearization and simplification can be expressed as [26]:

$$\begin{aligned}C_{i,j}^{n}\frac{h_{i,j}^{n+1/2}-h_{i,j}^{n}}{\Delta z_i}&=\frac{K_{i+1/2,j}^{n+1/2}\left(h_{i+1,j}^{n+1/2}-h_{i,j}^{n+1/2}\right)-K_{i-1/2,j}^{n+1/2}\left(h_{i,j}^{n+1/2}-h_{i-1,j}^{n+1/2}\right)}{(\Delta r)^2}\\&+\frac{K_{i,j}^{n+1/2}}{i\Delta r}\frac{\left(h_{i+1,j}^{n+1/2}-h_{i-1,j}^{n+1/2}\right)}{2\Delta r}+\frac{K_{i,j+1/2}^{n}\left(h_{i,j+1}^{n}-h_{i,j}^{n}\right)-K_{i,j-1/2}^{n}\left(h_{i,j}^{n}-h_{i,j-1}^{n}\right)}{(\Delta z)^2}\\&-\frac{\left(K_{i,j+1}^{n}-K_{i,j-1}^{n}\right)}{2\Delta z}-S_{i,j}^{n}\end{aligned} \tag{2}$$

In Eq. 2, superscript n refers to the current time step and superscript $n+1/2$ denotes the arithmetic mean of a parameter at time steps n and n+1. Furthermore, unsaturated hydraulic conductivity function (K) is defined by [27]:

$$K=K_s S_e^{\,l}\left[1-\left(1-S_e^{1/m}\right)^m\right]^2 \tag{3}$$

where K_s= saturated hydraulic conductivity [L/T], Se= effective saturation [-], m and l= shape parameters [-]. For K, we take the geometrical mean as proposed by Vauclin et al. [28].

$$K_{i+1/2,j}=\sqrt{K_{i+1,j}\times K_{i,j}} \tag{4}$$

$$K_{i-1/2,j}=\sqrt{K_{i-1,j}\times K_{i,j}} \tag{5}$$

It should be noted that third-type (Cauchy type) boundary condition is used to prescribe the water flux from point source (emitter) in the soil surface and a uniform constant water content has been used as initial condition in numerical scheme [29].

2.3. General overview of genetic programming

In this section, a brief overview of the GP and GEP is given. Detailed explanations of GP and GEP are provided by Koza [30] and Ferreira [31], respectively. GP was first proposed by Koza [30]. It is a generalization of genetic algorithms (GAs) [32]. The fundamental difference between GA, GP, and GEP is due to the nature of the individuals. In GA, the individuals are linear strings of fixed length (chromosomes). In GP, the individuals are nonlinear entities of different sizes and shapes (parse trees), and in GEP the individuals are encoded as linear strings of fixed length (the genome or chromosomes), which are afterwards expressed as nonlinear entities of different sizes and shapes [33,34]. GP is a search technique that allows for the solution of problems by automatically generating algorithms and expressions. These expressions are coded or represented as a tree structure with its terminals (leaves) and nodes (functions). GP applies GAs to a "population" of programs, typically encoded as tree-structures. Trial programs are evaluated against a "fitness function". Then the best solutions are selected for modification and re-evaluation. This modification-evaluation cycle is repeated until a "correct" program is produced.

There are five major preliminary steps for solving a problem by using GEP. These are the determination of (i) the set of terminals, (ii) the set of functions, (iii) the fitness measure, (iv) the values of the numerical parameters and qualitative variables for controlling the run, and (v) the criterion for designating a result and terminating a run [30]. A GEP flowchart improved by Ferreira [34] is presented in Figure 2. The automatic program generation is carried out by means of a process derived from Darwin's evolution theory, in which, after subsequent generations, new trees (individuals) are produced from old ones via crossover, copy, and mutation [35,36]. Based on natural selection, the best trees will have more chances of being chosen to become part of the next generation. Thus, a stochastic process is established where, after successive generations, a well-adapted tree is obtained.

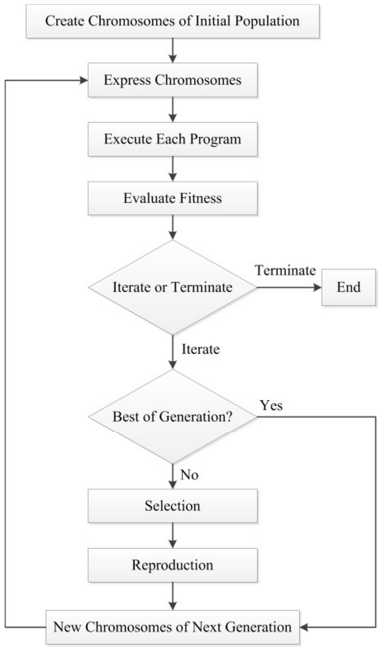

Figure 2. GEP flowchart improved by Ferreira [34]

There are five major steps in preparing to use GEP of which the first is to choose the fitness function. The fitness of an individual program i for fitness case j is evaluated by Ferreira [31] using:

$$If \quad E(ij) \le p, \quad then \quad f_{(ij)} = 1; \quad else \quad f_{(ij)} = 0 \tag{6}$$

Where p is the precision and E(ij) is the error of an individual program i for fitness case j. For the absolute error, this is expressed by:

$$E(ij) = \left| P_{(ij)} - T_j \right| \tag{7}$$

Again for the absolute error, the fitness f_i of an individual program i is expressed by:

$$f_i = \sum_{j=1}^{n} \left(R - \left| P_{(ij)} - T_j \right| \right) \tag{8}$$

Where R is the selection range, $P_{(ij)}$ is the value predicted by the individual program i for fitness case j (out of n fitness cases) and T_j is the target value for fitness case j. The second major step consists of choosing the set of terminals T and the set of functions F to create the chromosomes. In this problem, the terminal set obviously consists of the independent variables. But, the choice of the appropriate function set is not so obvious. However, a good guess can always be helpful in order to include all the necessary functions. In this study, six set of operators (Table 1) including different combinations of (+, -, ×, ÷, $\sqrt[3]{}$, $\sqrt{}$, ln, e^x, x^2, x^3, power, sine, cosine, arctangent) were utilized. The third major step is to choose the chromosomal architecture, i.e., the length of the head and the number of genes. Values of the length of the head, h = 8, and twelve genes per

Agriculture Science Developments Vol(3), No (5), May, 2014.

chromosome were employed for the present study. The fourth major step is to choose the linking function. In this study, the sub- programs were linked by addition. Finally, the fifth major step is to choose the set of genetic operators that cause variation along with their rates. A combination of all genetic operators, i.e., mutation, transposition and recombination, was used for this purpose. The parameters of the training of the GEP are given in Table 2.

Table 1. Combination of mathematical operators in GEP models

Model	Functions
GEP1	+, -, ×, ÷
GEP2	+, -, ×, ÷, ln, e^x
GEP3	+, -, ×, ÷, $\sqrt[3]{}$, $\sqrt{}$, x^2, x^3
GEP4	+, -, ×, ÷, $\sqrt[3]{}$, $\sqrt{}$, ln, e^x, x^2, x^3
GEP5	+, -, ×, ÷, $\sqrt[3]{}$, $\sqrt{}$, ln, e^x, x^2, x^3, sine, cosine, arctangent
GEP6	+, -, ×, ÷, $\sqrt[3]{}$, $\sqrt{}$, ln, e^x, x^2, x^3, power, sine, cosine, arctangent

Table 2. Parameters of the GEP model

Parameter	Value
Chromosomes	30
Head size	8
Number of Genes	12
Linking Function	Addition (+)
Mutation Rate	0.044
Inversion Rate	0.1
One-Point Recombination Rate	0.3
Two-Point Recombination Rate	0.3
Gene Recombination Rate	0.1
Gene Transposition Rate	0.1

2.4. M5 model tree

Model trees generalize the concepts of regression trees, which have constant values at their leaves [37]. So, they are analogous to piece-wise linear functions. M5 model tree [38] is a binary decision tree having linear regression function at the terminal (leaf) nodes, which can predict continuous numerical attributes. Tree-based models are constructed by a divide-and-conquer method. A model tree generation requires two different stages. The first stage involves using a splitting criterion to create a decision tree. The splitting criterion for the M5 model tree algorithm is based on treating the standard deviation of the class values that reach a node as a measure of the error at that node and calculating the expected reduction in this error as a result of testing each attribute at that node. The formula to compute the standard deviation reduction (SDR) is as follows:

$$SDR = s_d(T) - \sum \frac{|T_i|}{|T|} s_d(T_i) \tag{9}$$

where T represents a set of examples that reaches the node; T_i represents the subset of examples that have the i^{th} outcome of the potential set; and s_d represents the standard deviation. Due to the splitting process, the data in child nodes have less standard deviation as compared to the parent node and thus are more pure. After examining all the possible splits, M5 chooses the one that maximizes the expected error reduction. This division often produces a large tree like structure which may cause overfitting. To remove the problem of overfitting, the tree must be pruned back, for example by replacing a sub tree with a leaf. Thus, second stage in the design of model tree involves pruning the overgrown tree and replacing the sub trees with linear regression functions. This technique of generating the model tree splits the parameter space into areas (subspaces) and builds in each of them a linear regression model. For further details of M5 model tree, readers are referred to Quinlan [38].

2.5. Laboratory experiments

For evaluating the accuracy of the gene expression programming and M5 model trees, experiments of water infiltration under surface drip irrigation were conducted on a sandy soil (90% sand, 5% silt and 5% clay). Laboratory experiments were carried out using a 120 cm × 120 cm × 120 cm transparent Plexiglas box (as shown in Figure 3). The air dried sandy soil with a mean particle size d_{50} = 0.4 mm was compacted at predetermined dry bulk density of 1.5 $g.cm^{-3}$. A polyethylene pipeline connected to a water reservoir and laid on the soil surface, which had a 16 mm outside diameter and a wall thickness of 2 mm, was used for supplying the discharge rates of 2, 4 and 6 L/h. During operation, wetting pattern dimensions were measured using high performance photography and were analyzed by Digimizer Software. The observed soil wetting pattern had a high degree of horizontal symmetry.

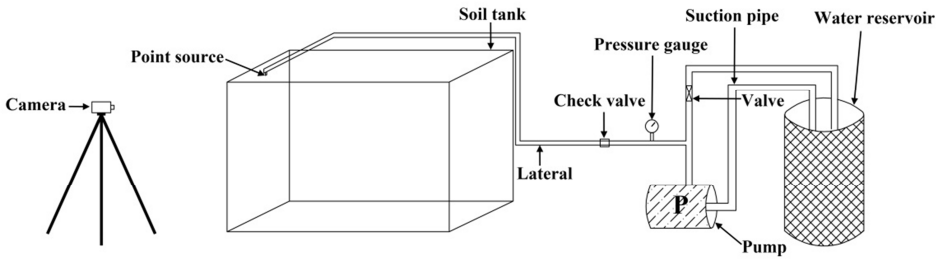

Figure 3. A schema of laboratory experiment

2.6. Evaluation parameters

Several parameters can be considered for the evaluation of radius (horizontal distance) and depth (vertical distance) of wetting pattern estimates. In this study the following statistic criteria were used: root mean squared error (RMSE), mean absolute error (MAE) and correlation coefficient (R^2).

$$RMSE = \sqrt{\frac{1}{n}\sum_{i=1}^{n}(d_m - d_s)^2} \tag{10}$$

$$MAE = \frac{1}{n}\sum_{i=1}^{n}|d_m - d_s| \tag{11}$$

$$R^2 = \frac{\left(\sum_{i=1}^{n} d_m d_s - \frac{1}{n}\sum_{i=1}^{n} d_m \sum_{i=1}^{n} d_s\right)^2}{\left(\sum_{i=1}^{n} {d_m}^2 - \frac{1}{n}\left(\sum_{i=1}^{n} d_m\right)^2\right)^2 \left(\sum_{i=1}^{n} {d_s}^2 - \frac{1}{n}\left(\sum_{i=1}^{n} d_s\right)^2\right)^2} \tag{12}$$

where d_m = distance from emitter computed by PNMCRE (cm), d_s = distance from emitter computed by different methods (cm) and n = number of values.

3. Results and discussion

In this research pore network modeling conjuncted by Richards' equation (PNMCRE) was used to compute the wetted soil depth and radius of 2160 simulated patterns using 10 sandy soils of various sand percentages. The precision of PNMCRE in estimating wetting patterns dimensions of drip irrigated sandy soil has been validated by Samadianfard et al. [39] by performing detailed laboratory experiments. In the current computations, emitter discharge ranged from 0.5 to 8 L/h and irrigation duration varied from 1 to 12 hrs. Then 1440 sets of these data were used for training and the rest were used for testing GEP and M5 model trees.

Six different combinations of mathematical operators in the GEP models and the M5 model trees were evaluated in the present study. Results of the statistical parameters for the studied methods in the test period are given in Table 3. Trigonometric functions were added into the function combinations of GEP5 and GEP6 to clarify the effect of circularity in depths and radius estimation of wetting patterns. From the Table it is clear that in the case of estimation of radius of wetting pattern, the circularity considerably increased GEP model's accuracy. For the GEP model, R^2 increases from 0.965 (for GEP1) to 0.967 (for GEP6) and similarly, RMSE and MAE indices decrease from 2.632 cm to 1.997 cm and from 2.133 cm to 1.548 cm, respectively. But the M5 model trees have better accuracy compared with the all GEP models. The M5 model trees by having R^2 value of 0.988, RMSE value of 1.286 and MAE value of 0.947 performed better than the all GEP models in estimation of wetting pattern's depth.

Accordingly in estimation of wetting pattern depth, by adding circularity functions, R^2 of the GEP increases from 0.927 to 0.944 and RMSE and MAE decrease from 7.342 cm to 6.420 cm and from 5.677 cm to 4.458 cm, respectively. Similar to the estimation of wetting pattern radius, M5 model trees have better accuracy compared with all the GEP models. M5 model trees by having R^2 value of 0.971, RMSE value of 6.127 and MAE value of 3.902 performed better than the all GEP models. Comparison of GEP and M5 model tree models indicates that the M5 model trees have a better accuracy than the all six models of GEP.

Table 3. Performance assessment of the GEP and M5 model tree methods in estimation of wetting pattern dimensions

Model	Estimation of radial distance (r)			Estimation of vertical distance (z)		
	RMSE	MAE	R^2	RMSE	MAE	R^2
GEP1	2.632	2.133	0.965	7.342	5.677	0.927
GEP2	3.126	2.535	0.962	7.346	5.181	0.929
GEP3	3.200	2.811	0.966	9.741	7.190	0.880
GEP4	2.158	1.797	0.961	6.736	4.897	0.942
GEP5	2.023	1.653	0.962	8.045	6.043	0.915
GEP6	1.997	1.548	0.967	6.420	4.458	0.944
M5 model tree	1.286	0.947	0.988	6.127	3.902	0.971

Agriculture Science Developments Vol(3), No (5), May, 2014.

Scatter plots of GEP6 (as the best GEP model) and M5 model trees for the estimation of radial distance from emitter (r) are shown in Figure 4. The estimates of the M5 model trees are closer to the corresponding observed values than those of the GEP model (Figure 4). In other words, the GEP model has much more scattered estimates than those of the M5 model trees. In Figure 4, the fit line equations (assuming that the equation is y=ax+b) given in the scatterplots indicate that the coefficients a and b of the M5 model trees are closer to the 1 and 0 than those of the GEP model, respectively. A comparison of the both models reveals that the estimates of the M5 model trees seem to be closer to the exact (1:1) line than the GEP model. On the other hand, in Figure 5 the scatter plots of vertical distances from emitter (z) estimated by the GEP6 and M5 model trees versus PNMCRE are illustrated. Similar to what reported for the radial distance from the emitter, the M5 model trees estimates of the vertical distance are closer to the observed values than those of the GEP model. However, both models underestimate the high vertical distance values. In similar researches, Hinnell et al. (2010) have used artificial neural network as one of the important branches of artificial intelligent methods for estimation of subsurface wetting patterns for drip irrigation. They reported the usefulness of artificial intelligent methods in water movement simulations. But to the best of our knowledge, there is not any published report of using M5 model tree in estimation of wetting patterns of drip irrigation.

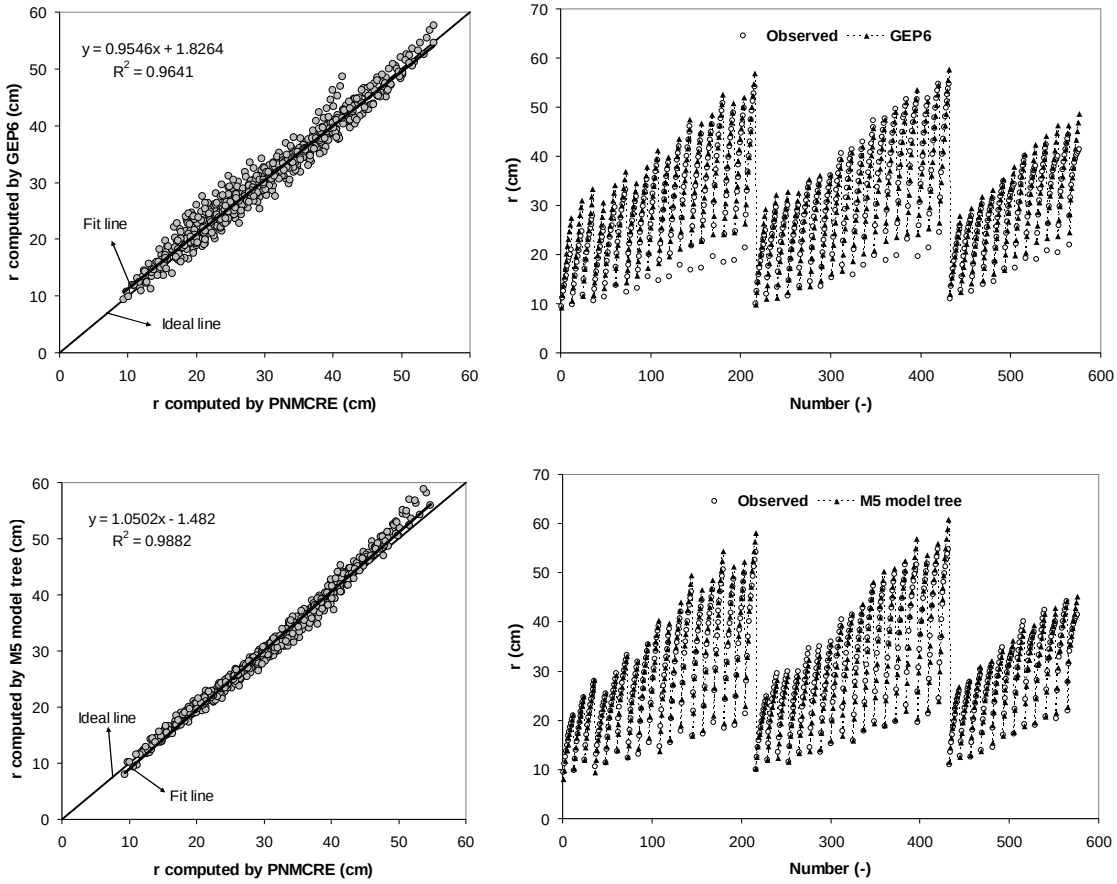

Figure 4. Radial distance from emitter (r) estimated by the GEP and M5 model tree methods versus PNMCRE in test period.

One of the advantages of GEP in comparison with other tools is producing analytical formula for determination of output parameters. After selecting GEP6, as the best GEP model, Eqs. (13) and (14) for determination of radius and depth of wetting patterns are resulted as:

$$r = 5.37537 + Q + T + (Clay \times Q \times T)^{1/3} + \theta_i + Q\sqrt{T \times \theta_i} + \cos\left[Q \times (6.63416 + Q) + (6.63416 + Clay) \times \theta_i^{\,2}\right] +$$

$$\sqrt{Sand \times T \times \theta_i} + \sqrt{\theta_i^{(0.656098 \times (2.19006 - \theta_i) + \cos[Q])^3}} + \cos\left[(-1.309 - \theta_i) \times (Clay + \theta_i) \times \sin[5.37537 + Clay]\right] + \arctan[Q] + \quad (13)$$

$$\arctan\left[(1.24716 - T)^2 (Ln[Q] - Silt \times Clay)\right] + \cos\left[Sand^{1/3}\right] + \cos\left[Clay + Q^{1/3} + Silt^3 - (1.50632/T)\right] +$$

$$\cos\left[0.171399 - Clay - \theta_i - Clay^2 \times \theta_i^{\,2}\right]$$

$$z = \left(-5.76727/T\right) + T \times Q^{\cos\left[Sand+\theta_i\right]^3} + \cos\left[Sand^{1/3} - \left(Clay \times Sand\right)^{1/3} + Sand \times \theta_i\right] + 4 \times \cos\left[Sand\right] +$$

$$\left(\theta_i + T \times \theta_i - 0.000298012 \times Clay^3\right) + \arctan\left[\left(Ln\left[Q\right] - Clay^3 - \left(2.17706/T\right)\right)/\theta_i\right] + T \times \sin\left[Q^{2/3}\right] + \theta_i + \quad (14)$$

$$\arctan\left[7.42389 - \left(7.27679/Q\right) - T + Ln\left[T\right]\right] + \sqrt{3.28861 \times Sand - 9.91571 \times Clay - \left(9.91571/\theta_i\right)} +$$

$$\cos\left[0.612159 \times T^{2/3} \times \arctan\left[0.2294 \times Clay\right]\right] + T \times \left(Q - \sin\left[8.59311 \times Sand - \theta_i\right]\right) +$$

$$\left(8.21368 + Sand\right) \times \sin\left[\theta_i\right] + \theta_i\left(2 \times \theta_i - \arctan\left[2.29578 - Q\right]\right)$$

where Sand= sand percentage [%], Silt= silt percentage [%], Clay= clay percentage [%], Q= emitter discharge rate [L/h], T= the time duration from the beginning of irrigation [h], θ_i= initial water content [-] and r, z= radial and vertical directions.

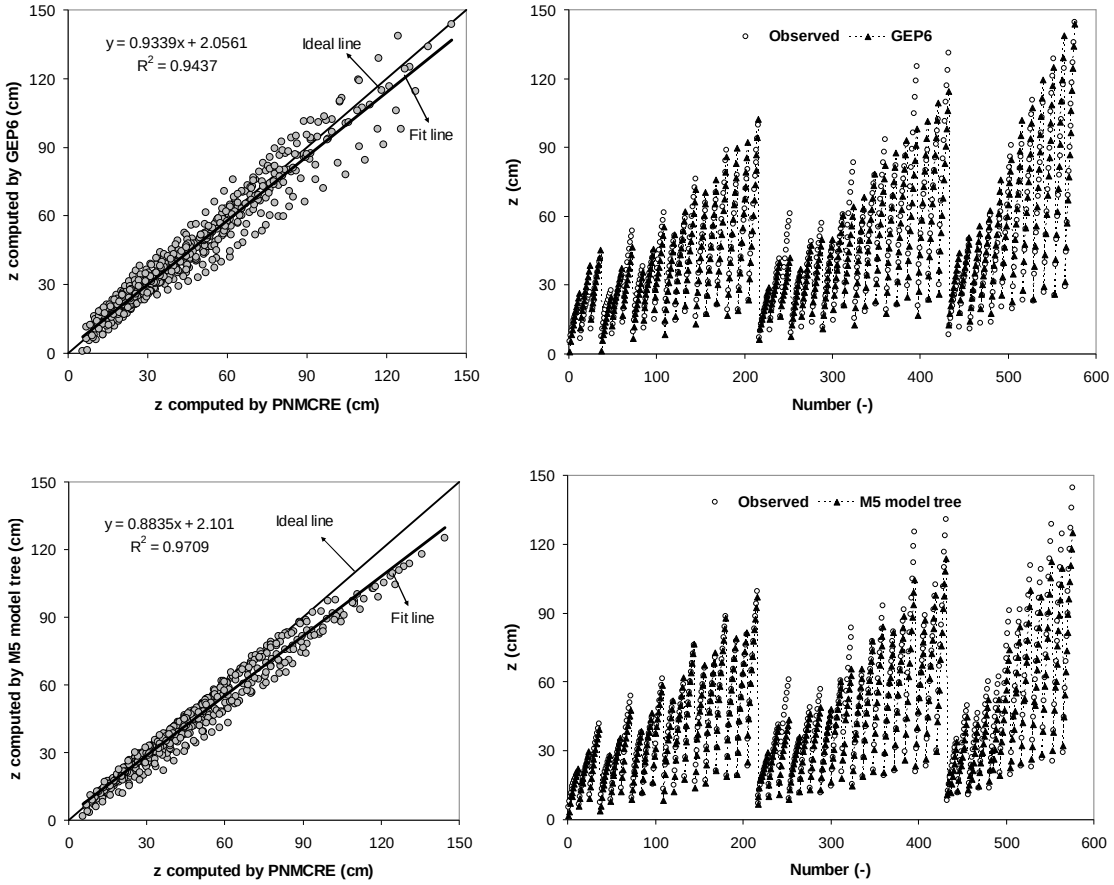

Figure 5. Vertical distance from emitter (z) estimated by the GEP and M5 model tree methods versus PNMCRE in test period.

Tables 4 and 5 provide linear relations by M5 model tree approach for estimation of radial distance from emitter and Tables 6 and 7 present correspondent relations for estimation of vertical distance. These equations can easily be used to predict the radial and vertical distance from emitter if the dataset is within the range of input parameters used to generate these equations.

Agriculture Science Developments Vol(3), No (5), May, 2014.

Table 4. Model tree for estimation of radial distance from emitter.

```
Q ≤ 3 :
|  T ≤ 4.5 :
|  |  T ≤ 1.5 : LM1
|  |  T >  1.5 :
|  |  |  Q ≤ 1.5 :
|  |  |  |  Silt ≤ 2.5 : LM2
|  |  |  |  Silt >  2.5 : LM3
|  |  |  Q >  1.5 : LM4
|  T >  4.5 :
|  |  Q ≤ 1.5 :
|  |  |  T ≤ 7.5 :
|  |  |  |  Silt ≤ 2.5 : LM5
|  |  |  |  Silt >  2.5 : LM6
|  |  |  T >  7.5 :
|  |  |  |  Silt ≤ 2.5 :
|  |  |  |  |  Q ≤ 0.75 :
|  |  |  |  |  |  θi ≤ 0.085 :
|  |  |  |  |  |  |  Sand ≤ 92.5 : LM7
|  |  |  |  |  |  |  Sand >  92.5 : LM8
|  |  |  |  |  |  θi >  0.085 : LM9
|  |  |  |  |  Q >  0.75 :
|  |  |  |  |  |  θi ≤ 0.08 :
|  |  |  |  |  |  |  Sand ≤ 92.5 : LM10
|  |  |  |  |  |  |  Sand >  92.5 :
|  |  |  |  |  |  |  |  Sand ≤ 97.5 : LM11
|  |  |  |  |  |  |  |  Sand >  97.5 : LM12
|  |  |  |  |  |  θi >  0.08 : LM13
|  |  |  |  Silt >  2.5 :
|  |  |  |  |  Q ≤ 0.75 :
|  |  |  |  |  |  θi ≤ 0.075 : LM14
|  |  |  |  |  |  θi >  0.075 : LM15
|  |  |  |  |  Q >  0.75 :
|  |  |  |  |  |  θi ≤ 0.08 : LM16
|  |  |  |  |  |  θi >  0.08 : LM17
|  |  Q >  1.5 :
|  |  |  T ≤ 7.5 :
|  |  |  |  Silt ≤ 2.5 :
|  |  |  |  |  θi ≤ 0.085 : LM18
|  |  |  |  |  θi >  0.085 : LM19
|  |  |  |  Silt >  2.5 : LM20
|  |  |  T >  7.5 :
|  |  |  |  Clay ≤ 2.5 : LM21
|  |  |  |  Clay >  2.5 :
|  |  |  |  |  Sand ≤ 87.5 :
|  |  |  |  |  |  θi ≤ 0.125 : LM22
|  |  |  |  |  |  θi >  0.125 : LM23
|  |  |  |  |  Sand >  87.5 : LM24
Q >  3 :
|  T ≤ 4.5 :
|  |  T ≤ 1.5 : LM25
|  |  T >  1.5 :
|  |  |  T ≤ 2.5 : LM26
|  |  |  T >  2.5 :
|  |  |  |  Silt ≤ 2.5 :
|  |  |  |  |  θi ≤ 0.085 : LM27
|  |  |  |  |  θi >  0.085 : LM28
|  |  |  |  Silt >  2.5 : LM29
|  T >  4.5 :
|  |  Clay ≤ 2.5 :
|  |  |  T ≤ 7.5 : LM30
|  |  |  T >  7.5 :
|  |  |  |  Q ≤ 5 : LM31
|  |  |  |  Q >  5 :
|  |  |  |  |  Sand ≤ 95 : LM32
|  |  |  |  |  Sand >  95 :
|  |  |  |  |  |  θi ≤ 0.068 : LM33
|  |  |  |  |  |  θi >  0.068 : LM34
|  |  Clay >  2.5 :
|  |  |  T ≤ 7.5 :
|  |  |  |  Q ≤ 5 :
|  |  |  |  |  Sand ≤ 87.5 : LM35
|  |  |  |  |  Sand >  87.5 : LM36
|  |  |  |  Q >  5 :
|  |  |  |  |  Sand ≤ 87.5 : LM37
|  |  |  |  |  Sand >  87.5 : LM38
|  |  |  T >  7.5 :
|  |  |  |  Q ≤ 5 :
|  |  |  |  |  Sand ≤ 87.5 :
|  |  |  |  |  |  θi ≤ 0.125 : LM39
|  |  |  |  |  |  θi >  0.125 : LM40
|  |  |  |  |  Sand >  87.5 : LM41
|  |  |  |  Q >  5 :
|  |  |  |  |  θi ≤ 0.12 :
|  |  |  |  |  |  Sand ≤ 87.5 : LM42
|  |  |  |  |  |  Sand >  87.5 : LM43
|  |  |  |  |  θi >  0.12 : LM44
```

Table 5. Linear models provided by M5 model tree for estimation of radial distance from emitter.

LM number	M5 model tree formulation
1	$r = 0.3611 \times Sand + 0.0207 \times Silt + 2.652 \times Q + 44.4134 \times \theta_i + 0.7759 \times T - 27.2013$
2	$r = 0.5109 \times Sand - 0.0064 \times Silt + 4.8972 \times Q + 78.0843 \times \theta_i + 2.2697 \times T - 46.3438$
3	$r = 0.4627 \times Sand - 0.0072 \times Silt + 4.4282 \times Q + 52.8625 \times \theta_i + 2.0308 \times T - 38.4494$
4	$r = 0.4635 \times Sand - 0.0151 \times Silt + 1.5017 \times Q + 64.1208 \times \theta_i + 2.6142 \times T - 36.3676$
5	$r = 0.5448 \times Sand - 0.0282 \times Silt + 7.2915 \times Q + 98.7061 \times \theta_i + 1.4499 \times T - 49.2805$
6	$r = 0.5465 \times Sand + 0.0012 \times Silt + 6.654 \times Q + 70.4551 \times \theta_i + 1.3355 \times T - 46.1756$
7	$r = 0.4244 \times Sand - 0.0394 \times Silt + 4.3478 \times Q + 75.3731 \times \theta_i + 1.0537 \times T - 32.3962$
8	$r = 0.4003 \times Sand - 0.0394 \times Silt + 4.3478 \times Q + 81.6651 \times \theta_i + 1.0432 \times T - 30.0394$
9	$r = 0.5646 \times Sand - 0.0394 \times Silt + 4.3478 \times Q + 109.3425 \times \theta_i + 1.0922 \times T - 47.9358$
10	$r = 0.3509 \times Sand - 0.0394 \times Silt + 4.3478 \times Q + 75.6924 \times \theta_i + 1.1317 \times T - 23.983$
11	$r = 0.2878 \times Sand - 0.0394 \times Silt + 4.3478 \times Q + 75.6924 \times \theta_i + 1.123 \times T - 17.3934$
12	$r = 0.2983 \times Sand - 0.0394 \times Silt + 4.3478 \times Q + 75.6924 \times \theta_i + 1.102 \times T - 18.3157$
13	$r = 0.5454 \times Sand - 0.0394 \times Silt + 4.3478 \times Q + 108.8089 \times \theta_i + 1.1805 \times T - 44.5479$
14	$r = 0.545 \times Sand - 0.0285 \times Silt + 3.8515 \times Q + 58.7912 \times \theta_i + 0.9821 \times T - 41.5276$
15	$r = 0.6171 \times Sand - 0.0204 \times Silt + 3.8515 \times Q + 82.1171 \times \theta_i + 1.0085 \times T - 49.5901$
16	$r = 0.5051 \times Sand - 0.0872 \times Silt + 3.8515 \times Q + 58.5369 \times \theta_i + 1.0676 \times T - 36.245$
17	$r = 0.5602 \times Sand - 0.0689 \times Silt + 3.8515 \times Q + 80.3902 \times \theta_i + 1.092 \times T - 42.8423$
18	$r = 0.2613 \times Sand - 0.1383 \times Silt + 0.8542 \times Q + 71.9148 \times \theta_i + 1.6592 \times T - 11.781$
19	$r = 0.4075 \times Sand - 0.1383 \times Silt + 0.8542 \times Q + 91.3564 \times \theta_i + 1.7342 \times T - 27.1724$
20	$r = 0.3889 \times Sand - 0.1545 \times Silt + 0.8542 \times Q + 74.7317 \times \theta_i + 1.6217 \times T - 23.8391$
21	$r = 0.3145 \times Sand - 0.0697 \times Silt + 0.0796 \times Clay + 0.8542 \times Q + 68.9255 \times \theta_i + 1.1614 \times T - 14.5524$
22	$r = 0.4172 \times Sand - 0.0697 \times Silt + 0.0724 \times Clay + 0.8542 \times Q + 90.4946 \times \theta_i + 1.4028 \times T - 27.134$
23	$r = 0.4172 \times Sand - 0.0697 \times Silt + 0.0724 \times Clay + 0.8542 \times Q + 85.9676 \times \theta_i + 1.4186 \times T - 26.5021$
24	$r = 0.6124 \times Sand - 0.0697 \times Silt + 0.0724 \times Clay + 0.8542 \times Q + 99.1093 \times \theta_i + 1.4224 \times T - 44.4238$
25	$r = 0.3593 \times Sand - 0.0754 \times Silt + 0.0078 \times Clay + 0.9624 \times Q + 58.8994 \times \theta_i + 1.1718 \times T - 24.6558$
26	$r = 0.3371 \times Sand - 0.1697 \times Silt + 0.0078 \times Clay + 1.1593 \times Q + 70.6014 \times \theta_i + 1.3287 \times T - 20.6857$
27	$r = 0.1674 \times Sand - 0.1258 \times Silt + 0.0078 \times Clay + 1.2986 \times Q + 61.1741 \times \theta_i + 3.2266 \times T - 8.0023$
28	$r = 0.4366 \times Sand - 0.1258 \times Silt + 0.0078 \times Clay + 1.3623 \times Q + 96.08 \times \theta_i + 3.5533 \times T - 36.8637$
29	$r = 0.3359 \times Sand - 0.1974 \times Silt + 0.0078 \times Clay + 1.2912 \times Q + 72.1272 \times \theta_i + 3.249 \times T - 24.6448$
30	$r = 0.1868 \times Sand - 0.0239 \times Silt + 0.0538 \times Clay + 1.2315 \times Q + 64.4107 \times \theta_i + 1.6331 \times T - 5.3395$
31	$r = 0.066 \times Sand - 0.0239 \times Silt + 0.0538 \times Clay + 0.5999 \times Q + 51.7842 \times \theta_i + 1.149 \times T + 12.8465$
32	$r = 0.098 \times Sand - 0.0239 \times Silt + 0.0538 \times Clay + 1.2276 \times Q + 53.0972 \times \theta_i + 1.2239 \times T + 7.3016$
33	$r = -0.0196 \times Sand - 0.0239 \times Silt + 0.0538 \times Clay + 0.7393 \times Q - 2.1393 \times \theta_i + 0.8943 \times T + 27.0725$
34	$r = -0.0196 \times Sand - 0.0239 \times Silt + 0.0538 \times Clay + 0.7393 \times Q - 2.1393 \times \theta_i + 0.8298 \times T + 27.4798$
35	$r = 0.5948 \times Sand - 0.0239 \times Silt + 0.0519 \times Clay + 0.9922 \times Q + 100.5273 \times \theta_i + 2.3298 \times T - 46.1032$
36	$r = 0.7159 \times Sand - 0.0239 \times Silt + 0.0519 \times Clay + 0.9922 \times Q + 107.3673 \times \theta_i + 2.3405 \times T - 56.9576$
37	$r = 0.4747 \times Sand - 0.0239 \times Silt + 0.0519 \times Clay + 1.6489 \times Q + 103.0795 \times \theta_i + 2.4715 \times T - 39.122$
38	$r = 0.6004 \times Sand - 0.0239 \times Silt + 0.0519 \times Clay + 1.6337 \times Q + 111.5023 \times \theta_i + 2.4765 \times T - 49.6064$
39	$r = 0.4605 \times Sand - 0.0239 \times Silt + 0.0519 \times Clay + 0.8292 \times Q + 107.0663 \times \theta_i + 1.7564 \times T - 30.3567$
40	$r = 0.4605 \times Sand - 0.0239 \times Silt + 0.0519 \times Clay + 0.8292 \times Q + 101.7386 \times \theta_i + 1.7745 \times T - 29.5976$
41	$r = 0.5165 \times Sand - 0.0239 \times Silt + 0.0519 \times Clay + 0.8292 \times Q + 111.1883 \times \theta_i + 1.7532 \times T - 34.0449$
42	$r = 0.388 \times Sand - 0.0239 \times Silt + 0.0519 \times Clay + 1.81 \times Q + 97.8911 \times \theta_i + 1.8478 \times T - 27.3328$
43	$r = 0.2756 \times Sand - 0.0239 \times Silt + 0.0519 \times Clay + 1.8136 \times Q + 77.7597 \times \theta_i + 1.8017 \times T - 12.8904$
44	$r = 0.7767 \times Sand - 0.0239 \times Silt + 0.0519 \times Clay + 1.8715 \times Q + 71.99 \times \theta_i + 1.9464 \times T - 57.0072$

Agriculture Science Developments Vol(3), No (5), May, 2014.

Table 6. Model tree for estimation of vertical distance from emitter.

```
Q ≤ 3 :
| T ≤ 4.5 :
| | T ≤ 1.5 : LM1
| | T > 1.5 :
| | | Sand ≤ 92.5 : LM2
| | | Sand > 92.5 : LM3
| T > 4.5 :
| | Sand ≤ 92.5 :
| | | Q ≤ 1.5 :
| | | | θi ≤ 0.08 :
| | | | | Q ≤ 0.75 : LM4
| | | | | Q > 0.75 :
| | | | | | T ≤ 7.5 : LM5
| | | | | | T > 7.5 :
| | | | | | | Sand ≤ 87.5 : LM6
| | | | | | | Sand > 87.5 : LM7
| | | | θi > 0.08 :
| | | | | T ≤ 7.5 :
| | | | | | Sand ≤ 87.5 : LM8
| | | | | | Sand > 87.5 :
| | | | | | | Silt ≤ 5 : LM9
| | | | | | | Silt > 5 : LM10
| | | | | T > 7.5 :
| | | | | | Sand ≤ 87.5 :
| | | | | | | θi ≤ 0.11 :
| | | | | | | | Q ≤ 0.75 :
| | | | | | | | | Silt ≤ 10 : LM11
| | | | | | | | | Silt > 10 : LM12
| | | | | | | | Q > 0.75 :
| | | | | | | | | Silt ≤ 10 : LM13
| | | | | | | | | Silt > 10 : LM14
                                | | | | | | | θi > 0.11 :
| | | | | | | | Q ≤ 0.75 : LM15
| | | | | | | | Q > 0.75 :
| | | | | | | | | Silt ≤ 10 : LM16
| | | | | | | | | Silt > 10 : LM17
| | | | | | Sand > 87.5 :
| | | | | | | Silt ≤ 5 :
| | | | | | | | θi ≤ 0.115 :
| | | | | | | | | Q ≤ 0.75 : LM18
| | | | | | | | | Q > 0.75 : LM19
| | | | | | | | θi > 0.115 : LM20
| | | | | | | Silt > 5 : LM21
| | | Q > 1.5 :
| | | | θi ≤ 0.09 :
| | | | | T ≤ 7.5 : LM22
| | | | | T > 7.5 :
| | | | | | Sand ≤ 87.5 : LM23
| | | | | | Sand > 87.5 : LM24
| | | | θi > 0.09 :
| | | | | T ≤ 8.5 :
| | | | | | Sand ≤ 87.5 :
| | | | | | | θi ≤ 0.115 : LM25
| | | | | | | θi > 0.115 : LM26
| | | | | | Sand > 87.5 :
| | | | | | | Silt ≤ 5 :
| | | | | | | | θi ≤ 0.12 : LM27
| | | | | | | | θi > 0.12 : LM28
| | | | | | | Silt > 5 : LM29
| | | | | T > 8.5 :
| | | | | | Sand ≤ 87.5 :
| | | | | | | θi ≤ 0.115 :
| | | | | | | | Silt ≤ 10 : LM30
| | | | | | | | Silt > 10 : LM31
| | | | | | | θi > 0.115 :
| | | | | | | | Silt ≤ 10 : LM32
| | | | | | | | Silt > 10 : LM33
| | | | | | Sand > 87.5 :
| | | | | | | Silt ≤ 5 :
| | | | | | | | θi ≤ 0.12 : LM34
| | | | | | | | θi > 0.12 : LM35
| | | | | | | Silt > 5 : LM36
| | Sand > 92.5 :
| | | Q ≤ 1.5 :
| | | | T ≤ 7.5 : LM37
| | | | T > 7.5 :
| | | | | θi ≤ 0.063 :
| | | | | | Sand ≤ 97.5 : LM38
| | | | | | Sand > 97.5 :
| | | | | | | Q ≤ 0.75 : LM39
| | | | | | | Q > 0.75 : LM40
| | | | | θi > 0.063 : LM41
| | | Q > 1.5 : LM42
Q > 3 :
| T ≤ 4.5 :
| | T ≤ 1.5 : LM43
| | T > 1.5 :
| | | Sand ≤ 92.5 : LM44
| | | Sand > 92.5 : LM45
| T > 4.5 :
| | Sand ≤ 92.5 :
| | | T ≤ 7.5 :
| | | | Q ≤ 5 : LM46
| | | | Q > 5 :
| | | | | θi ≤ 0.105 :
| | | | | | Sand ≤ 87.5 : LM47
| | | | | | Sand > 87.5 : LM48
| | | | | θi > 0.105 : LM49
| | | T > 7.5 :
| | | | Q ≤ 5 :
| | | | | θi ≤ 0.09 :
| | | | | | Sand ≤ 87.5 : LM50
| | | | | | Sand > 87.5 : LM51
| | | | | θi > 0.09 :
| | | | | | Sand ≤ 87.5 :
| | | | | | | θi ≤ 0.12 : LM52
| | | | | | | θi > 0.12 :
| | | | | | | | Silt ≤ 10 : LM53
| | | | | | | | Silt > 10 : LM54
| | | | | | Sand > 87.5 :
| | | | | | | Silt ≤ 5 :
| | | | | | | | θi ≤ 0.12 : LM55
| | | | | | | | θi > 0.12 : LM56
| | | | | | | Silt > 5 : LM57
| | | | Q > 5 :
| | | | | Sand ≤ 87.5 :
| | | | | | θi ≤ 0.12 :
| | | | | | | T ≤ 9.5 : LM58
| | | | | | | T > 9.5 : LM59
| | | | | | θi > 0.12 : LM60
| | | | | Sand > 87.5 :
| | | | | | θi ≤ 0.105 :
| | | | | | | Silt ≤ 5 : LM61
| | | | | | | Silt > 5 :
| | | | | | | | θi ≤ 0.065 : LM62
| | | | | | | | θi > 0.065 : LM63
| | | | | | θi > 0.105 : LM64
| | Sand > 92.5 :
| | | T ≤ 7.5 :
| | | | Sand ≤ 97.5 : LM65
| | | | Sand > 97.5 : LM66
| | | T > 7.5 :
| | | | Sand ≤ 97.5 :
| | | | | θi ≤ 0.075 :
| | | | | | Q ≤ 5 : LM67
| | | | | | Q > 5 : LM68
| | | | | θi > 0.075 : LM69
| | | | Sand > 97.5 :
| | | | | Q ≤ 5 :
| | | | | | θi ≤ 0.063 : LM70
| | | | | | θi > 0.063 : LM71
| | | | | Q > 5 :
| | | | | | T ≤ 9.5 : LM72
| | | | | | T > 9.5 : LM73
```

Table 7. Linear models provided by M5 model tree for estimation of vertical distance from emitter.

LM number	M5 model tree formulation
1	$z = 0.9741 \times Sand + 0.1499 \times Silt + 4.0118 \times Q + 83.7405 \times \theta_i + 1.3653 \times T - 89.9932$
2	$z = 1.5304 \times Sand + 0.408 \times Silt + 5.5473 \times Q + 122.292 \times \theta_i + 3.6172 \times T - 147.0102$
3	$z = 1.7985 \times Sand + 0.1943 \times Silt + 6.494 \times Q + 262.2769 \times \theta_i + 4.1681 \times T - 184.5463$
4	$z = 1.5267 \times Sand + 0.2828 \times Silt + 6.0032 \times Q + 70.0759 \times \theta_i + 1.7082 \times T - 137.4801$
5	$z = 1.5934 \times Sand + 0.3115 \times Silt + 6.0032 \times Q + 70.0759 \times \theta_i + 1.9542 \times T - 142.7336$
6	$z = 1.5621 \times Sand + 0.327 \times Silt + 6.0032 \times Q + 70.0759 \times \theta_i + 1.8447 \times T - 139.5114$
7	$z = 1.5621 \times Sand + 0.3552 \times Silt + 6.0032 \times Q + 70.0759 \times \theta_i + 1.8897 \times T - 139.4849$
8	$z = 1.9662 \times Sand + 0.7448 \times Silt + 9.7913 \times Q + 203.1932 \times \theta_i + 2.3952 \times T - 196.0608$
9	$z = 2.0689 \times Sand + 0.7942 \times Silt + 8.9618 \times Q + 249.8931 \times \theta_i + 2.5532 \times T - 207.3174$
10	$z = 2.0689 \times Sand + 0.8543 \times Silt + 8.1518 \times Q + 222.378 \times \theta_i + 2.6035 \times T - 203.4525$
11	$z = 1.8 \times Sand + 0.7753 \times Silt + 10.4183 \times Q + 177.4083 \times \theta_i + 2.0259 \times T - 178.3107$
12	$z = 1.8 \times Sand + 0.7753 \times Silt + 10.4183 \times Q + 177.4083 \times \theta_i + 2.0334 \times T - 178.2681$
13	$z = 1.8 \times Sand + 0.778 \times Silt + 10.4183 \times Q + 177.4083 \times \theta_i + 2.0625 \times T - 178.0753$
14	$z = 1.8 \times Sand + 0.778 \times Silt + 10.4183 \times Q + 177.4083 \times \theta_i + 2.0731 \times T - 178.0537$
15	$z = 1.8 \times Sand + 0.7803 \times Silt + 11.0003 \times Q + 177.4083 \times \theta_i + 2.1639 \times T - 177.7758$
16	$z = 1.8 \times Sand + 0.8064 \times Silt + 11.0003 \times Q + 177.4083 \times \theta_i + 2.21 \times T - 177.7673$
17	$z = 1.8 \times Sand + 0.8064 \times Silt + 11.0003 \times Q + 177.4083 \times \theta_i + 2.2236 \times T - 177.7097$
18	$z = 1.9358 \times Sand + 0.8607 \times Silt + 10.532 \times Q + 277.8001 \times \theta_i + 2.2365 \times T - 197.919$
19	$z = 1.9358 \times Sand + 0.8607 \times Silt + 10.532 \times Q + 277.8001 \times \theta_i + 2.2462 \times T - 197.8545$
20	$z = 1.9358 \times Sand + 0.8607 \times Silt + 10.3613 \times Q + 277.8001 \times \theta_i + 2.3092 \times T - 197.2407$
21	$z = 1.9358 \times Sand + 0.9838 \times Silt + 9.3949 \times Q + 247.8923 \times \theta_i + 2.3685 \times T - 193.1382$
22	$z = 2.1929 \times Sand + 0.4433 \times Silt + 2.2924 \times Q + 106.2225 \times \theta_i + 2.6157 \times T - 193.7621$
23	$z = 2.1373 \times Sand + 0.4613 \times Silt + 2.2924 \times Q + 106.2225 \times \theta_i + 2.4743 \times T - 188.327$
24	$z = 2.1373 \times Sand + 0.4894 \times Silt + 2.2924 \times Q + 106.2225 \times \theta_i + 2.5344 \times T - 188.064$
25	$z = 2.72 \times Sand + 0.8359 \times Silt + 2.2924 \times Q + 208.3433 \times \theta_i + 3.0277 \times T - 253.4088$
26	$z = 2.72 \times Sand + 0.8343 \times Silt + 2.2924 \times Q + 208.3433 \times \theta_i + 3.0767 \times T - 253.1746$
27	$z = 2.8178 \times Sand + 0.921 \times Silt + 2.2924 \times Q + 246.254 \times \theta_i + 3.191 \times T - 265.0254$
28	$z = 2.8178 \times Sand + 0.921 \times Silt + 2.2924 \times Q + 246.254 \times \theta_i + 3.2059 \times T - 264.9469$
29	$z = 2.8178 \times Sand + 0.9564 \times Silt + 2.2924 \times Q + 238.0419 \times \theta_i + 3.2443 \times T - 264.0076$
30	$z = 2.967 \times Sand + 0.9466 \times Silt + 2.2924 \times Q + 230.1341 \times \theta_i + 2.8005 \times T - 276.5447$
31	$z = 2.967 \times Sand + 0.9466 \times Silt + 2.2924 \times Q + 230.1341 \times \theta_i + 2.8075 \times T - 276.5261$
32	$z = 2.967 \times Sand + 0.9463 \times Silt + 2.2924 \times Q + 230.1341 \times \theta_i + 2.8411 \times T - 276.2501$
33	$z = 2.967 \times Sand + 0.9463 \times Silt + 2.2924 \times Q + 230.1341 \times \theta_i + 2.8478 \times T - 276.2299$
34	$z = 3.1014 \times Sand + 1.0719 \times Silt + 2.2924 \times Q + 280.7476 \times \theta_i + 2.9636 \times T - 292.6596$
35	$z = 3.1014 \times Sand + 1.0719 \times Silt + 2.2924 \times Q + 280.7476 \times \theta_i + 2.9771 \times T - 292.567$
36	$z = 3.1014 \times Sand + 1.1219 \times Silt + 2.2924 \times Q + 269.7918 \times \theta_i + 3.0189 \times T - 291.3783$
37	$z = 3.7997 \times Sand + 0.1603 \times Silt + 11.8672 \times Q + 587.8622 \times \theta_i + 3.5375 \times T - 403.0206$
38	$z = 3.6969 \times Sand + 0.1603 \times Silt + 14.9008 \times Q + 484.7238 \times \theta_i + 3.1101 \times T - 387.2816$
39	$z = 3.6138 \times Sand + 0.1603 \times Silt + 15.8261 \times Q + 484.7238 \times \theta_i + 3.2051 \times T - 379.6853$
40	$z = 3.6138 \times Sand + 0.1603 \times Silt + 15.8261 \times Q + 484.7238 \times \theta_i + 3.2255 \times T - 379.5801$
41	$z = 4.6594 \times Sand + 0.1603 \times Silt + 14.6377 \times Q + 688.0277 \times \theta_i + 3.388 \times T - 494.758$
42	$z = 5.4734 \times Sand + 0.1603 \times Silt + 5.629 \times Q + 716.5303 \times \theta_i + 4.3658 \times T - 567.8808$
43	$z = 1.5495 \times Sand + 0.2171 \times Silt + 1.8669 \times Q + 103.8621 \times \theta_i + 2.5127 \times T - 141.9226$
44	$z = 2.3322 \times Sand + 0.6011 \times Silt + 2.5708 \times Q + 157.6012 \times \theta_i + 7.0905 \times T - 225.7162$
45	$z = 3.407 \times Sand + 0.2931 \times Silt + 3.1047 \times Q + 338.9301 \times \theta_i + 9.8066 \times T - 352.0708$
46	$z = 3.311 \times Sand + 0.9383 \times Silt + 1.927 \times Q + 226.6934 \times \theta_i + 4.6956 \times T - 310.2196$
47	$z = 2.6043 \times Sand + 0.9224 \times Silt + 3.5403 \times Q + 216.5708 \times \theta_i + 5.1072 \times T - 257.5366$
48	$z = 2.6043 \times Sand + 1.1697 \times Silt + 3.581 \times Q + 267.6827 \times \theta_i + 5.513 \times T - 261.9307$

Finally in order to better demonstrate the capability of the M5 model tree in comparison with GEP, the experimental and simulated wetted patterns for a sandy soil with an emitter discharge of 4 L/h are shown in Figure 6. The patterns are for the time duration of 1, 2, 3, 4, 5 and 6 h from the beginning of irrigation. The M5 model tree data are closer to the observed wetting patterns than those of the GEP6 for irrigation durations less than 4 h (Figure 6). The estimated depth of wetting patterns with both M5 model tree and GEP6 are not in very good agreement with the observed depths. In other words, both mentioned models overestimated the depth of wetting patterns. In overall, it can be concluded that the M5 model tree has better performance than GEP6 in estimation of wetting pattern's dimensions.

Agriculture Science Developments Vol(3), No (5), May, 2014.

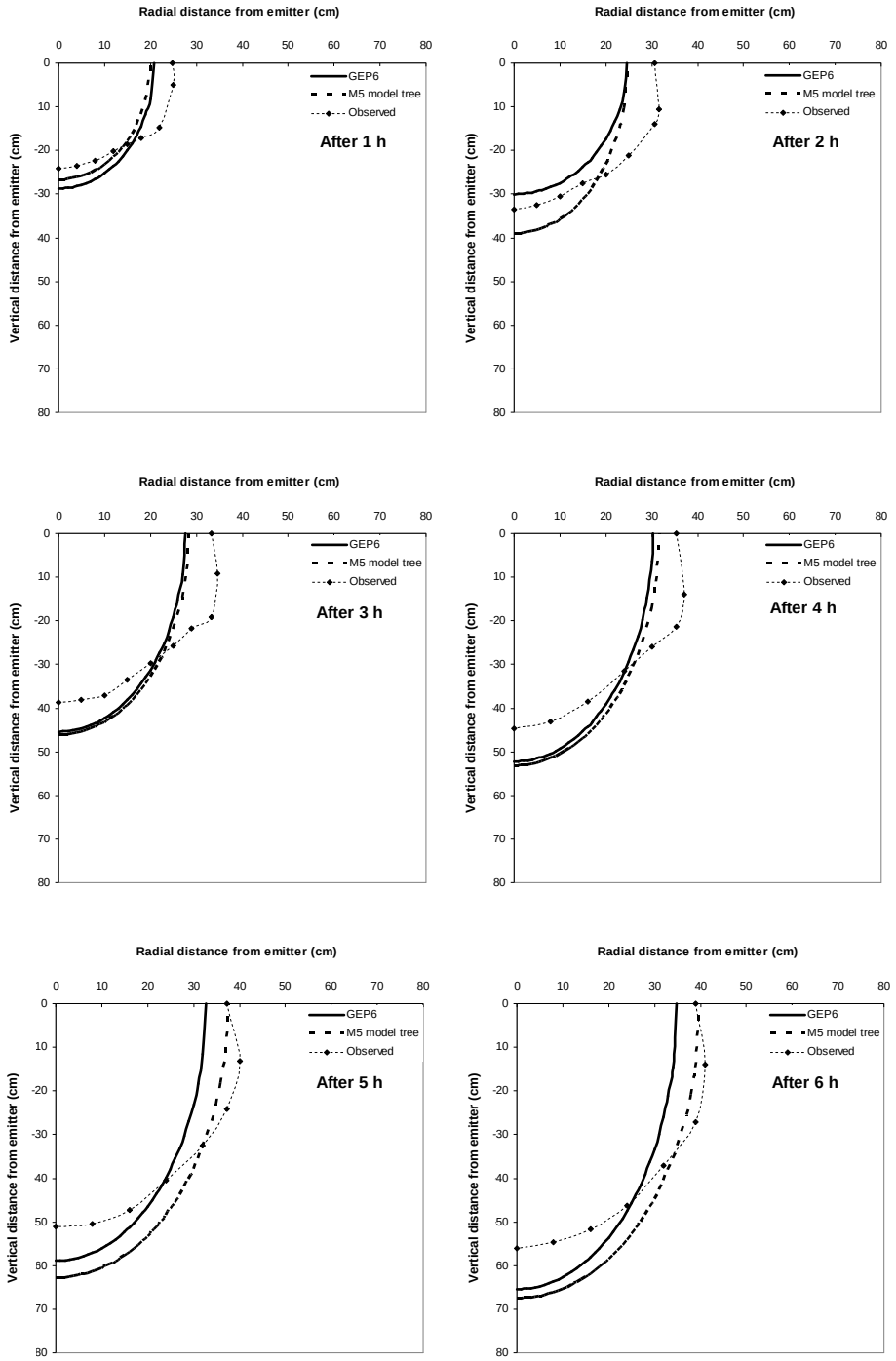

Figure 6. Experimental and simulated wetted patterns by the GEP and M5 model tree methods for a sandy soil with an emitter discharge of 4 L/h

4. Conclusions

The M5 model tree and gene expression programming were used to simulate wetting patterns of drip irrigation systems and the results were compared. The results are satisfactory and allow the users to estimate wetting patterns dimensions for any given time, emitter discharges and soil hydraulic properties needles to perform a detailed numerical simulation using the pore network modelling. The M5 model tree was found to be better than the GEP models at all simulated cases. The comparison of all irrigation treatments with laboratory experiments revealed that the M5 model tree could be employed successfully in modeling wetting patterns of drip irrigation.

Acknowledgements

The authors gratefully acknowledge the financial support by the Research Department of the University of Tabriz.

References

[1] Arbat G, Puig-Bargues J, Barragan J, Bonany J, Ramirez de Cartagena F. (2008). Monitoring soil water status for micro-irrigation management versus modelling approach. Biosystems Engineering, 100(2): 286-296.
[2] Singh DK, Rajput TBS, Singh DK, Sikarwar HS, Sahoo RN, Ahmad T. (2006). Simulation of soil wetting pattern with subsurface drip irrigation from line source. Agricultural Water Management, 83: 130-134.
[3] Mmolawa K, Or D. (2000). Water and solute dynamics under a drip irrigated crop: experiments and analytical model. Transaction ASAE, 43:1597-1608.
[4] Philip JR. (1968). Steady infiltration from buried point sources and spherical cavities. Water Resource Research, 4(5): 1039-1047.
[5] Ben-Asher J, Phene CJ. (1993). Analysis of surface and subsurface drip irrigation using a numerical model. In: Subsurface Drip Irrigation - Theory, Practices and Application, California State University, Fresno, CA, pp. 185-202. CATI Pub. No. 92 1001.
[6] Taghavi SA, Marino Miguel A, Rolston DE. (1984). Infiltration from trickle-irrigation source. Journal of Irrigation and Drainage Engineering-ASCE, 10: 331-341.
[7] Healy RW. (1987). Simulation of trickle-irrigation, an extension to U.S. Geological Survey's computer program Vs 2D. US Geological Survey Water Resour Invest 87-4086, US Govt Washington, DC.
[8] Skaggs TH, Trout TJ, Simunek J, Shouse PJ. (2004). Comparison of Hydrus-2D simulations of drip irrigation with experimental observations. Journal of Irrigation and Drainage Engineering-ASCE, 130(4): 304-310.
[9] Zhou Q, Kang S, Zhang L, Li F. (2007). Comparison of APRI and Hydrus-2D models to simulate soil water dynamics in a vineyard under alternate partial root zone drip irrigation. Plant and Soil, 291: 211-223.
[10] Li J, Zhang J, Rao M. (2005). Modeling of water flow and nitrogen transport under surface drip fertigation. Transaction ASAE, 48: 627-637.
[11] Celia MA, Reeves PC, Ferrand LA. (1995). Recent advances in pore scale models for multiphase flow in prous media. Review of Geophysics, 33 (S1): 1049-1058.
[12] Blunt M, Jackson MD, Piri M, Valvatne PH. (2002). Detailed physics, predictive capabilities and macroscopic consequences for pore-network models of multiphase flow. Advances in Water Recourses, 25: 1069-1089.
[13] Held RJ, Celia MA. (2001). Modeling support of functional relationships between capillary pressure, saturation, interfacial area and common lines. Advances in Water Resources, 24: 325-343.
[14] Joekar-Niasar V, Hassanizadeh SM, Leijnse A. (2008). Insights into the relationships among capillary pressure, saturation, interfacial area and relative permeability using pore-network modeling. Transport in Porous Media, 74(2): 201-219.
[15] Banzhaf W, Nordin P, Keller RE, Francone FD. (1998). Genetic programming. Morgan Kaufmann, San Francisco, CA.
[16] Kisi O, Guven A. (2010). Evapotranspiration modeling using linear genetic programming technique. Journal of Irrigation and Drainage Engineering-ASCE, 136(10): 715-723.
[17] Samadianfard S. (2012). Gene expression programming analysis of implicit Colebrook-White equation in turbulent flow friction factor calculation. Journal of Petroleum Science and Engineering, 92-93: 48-55.
[18] Samadianfard S, Delirhasannia R, Kisi O, Agirre-Basurko E. (2013). Comparative analysis of ozone level prediction models using gene expression programming and multiple linear regression. GEOFIZIKA, 30: 43-74.
[19] Solomatine DP, Xue Y. (2004). M5 Model Trees and Neural Networks: Application to Flood Forecasting in the Upper Reach of the Huai River in China. Journal of Hydrologic Engineering-ASCE, 9(6): 491-501.
[20] Bhattacharya B, Solomatine DP. (2006). Machine learning in sedimentation modeling. Neural Networks, 19: 208-214.
[21] Stravs L, Brilly M. (2007). Development of a low flow forecasting model using the M5 machine learning method. Hydrological Science Journal, 52(3): 466-477.
[22] Ditthakit P, Chinnarasri C. (2012). Estimation of Pan Coefficient using M5 Model Tree. American Journal of Environmental Sciences, 8(2): 95-103.
[23] Hinnell AC, Lazarovitch N, Furman A, Poulton M, Warrick AW. (2010). Neuro-Drip: estimation of subsurface wetting patterns for drip irrigation using neural networks. Irrigation Science, 28:535-544.
[24] Joekar-Niasar V, Hassanizadeh SM, Dahle HK. (2010). Non-equilibrium effects in capillarity and interfacial area in two-phase flow: dynamic pore-network modelling. Journal of Fluid Mechanics, 655: 38-71.
[25] Bear J. (1988). Dynamics of Fluids in Porous Media, Dover Publications, New York.
[26] Besharat S, Nazemi AH, Sadraddini AA. (2010). Parametric modeling of root length density and root water uptake in unsaturated soil. Turkish Journal of Agricultural & Foresty, 34: 439-449.
[27] Van Genuchten MTh. (1980). A closed-form equation for predicting the hydraulic conductivity of unsaturated soils. Soil Science Society of American Journal, 44: 892-898.
[28] Vauclin M, Haverkamp R, Vauchaud G. (1989). Résolution de l'équation de l'infiltration de l'eau dans le sol : approches analytiques et numériques. Presses Universitaires de Grenoble, Grenoble, 183 pp.
[29] Shan Y, Wang Q. (2012). Simulation of salinity distribution in the overlap zone with double-point-source drip irrigation using HYDRUS-3D. Australian Journal of Crop Science, 6(2): 238-247.
[30] Koza JR. (1992). Genetic programming, on the programming of computers by means of natural selection. MIT Press, Cambridge, MA, USA.
[31] Ferreira C. (2006). Gene expression programming: mathematical modeling by an artificial intelligence. Springer, Berlin, 478 pp.
[32] Goldberg DE. (1989). Genetic algorithms in search, optimization, and machine learning. Addison-Wesley, Reading, MA, USA.
[33] Ferreira C. (2001a). Gene expression programming in problem solving. 6th Online World Conf on Soft Computing in Industrial Applications (invited tutorial), Springer, Berlin (Germany). pp: 1-22.
[34] Ferreira C. (2001b). Gene expression programming: A new adaptive algorithm for solving problems. Complex Systems, 13(2): 87-129.
[35] Fuchs M. (1998). Crossover versus mutation: An empirical and theoretical case study. Proc. 3rd Ann Conf on Genetic Programming, Morgan- Kauffman, San Mateo, CA, (USA), Jul 22-25. pp: 78-85.
[36] Luke S, Spector L. (1998). A revised comparison of crossover and mutation in genetic programming. Proc 3rd Ann Conf on Genetic Programming, Morgan-Kauffman, Madison, San Mateo, CA, USA.
[37] Witten IH, Frank E. (2005). Data Mining: Practical Machine Learning Tools and Techniques with Java Implementations. Morgan Kaufmann: San Francisco.
[38] Quinlan JR. (1992). Learning with continuous classes. In: Proc. AI'92 (Fifth Australian Joint Conf. on Artificial Intelligence) (ed. by A. Adams & L. Sterling), 343–348. World Scientific, Singapore.
[39] Samadianfard S, Sadraddini AA, Nazemi AH. (2013). Numerical and experimental analyses of a sandy soil water movement under a point source using dynamic pore network modeling. Journal of Applied Biological Science , 7(3): 90-98.